

Correcting lateral chromatic aberrations in non-monochromatic X-ray microscopy

Ken Vidar Falch, Carsten Detlefs, Marco Di Michiel, Irina Snigireva, Anatoly Snigirev, and Ragnvald H. Mathiesen

Citation: [Applied Physics Letters](#) **109**, 054103 (2016); doi: 10.1063/1.4960193

View online: <http://dx.doi.org/10.1063/1.4960193>

View Table of Contents: <http://scitation.aip.org/content/aip/journal/apl/109/5?ver=pdfcov>

Published by the [AIP Publishing](#)

Articles you may be interested in

[Soft x-ray holographic microscopy](#)

Appl. Phys. Lett. **96**, 042501 (2010); 10.1063/1.3291942

[The X-ray Microscopy Project at Saga LS](#)

AIP Conf. Proc. **716**, 152 (2004); 10.1063/1.1796604

[X-ray Holographic Microscopy in China](#)

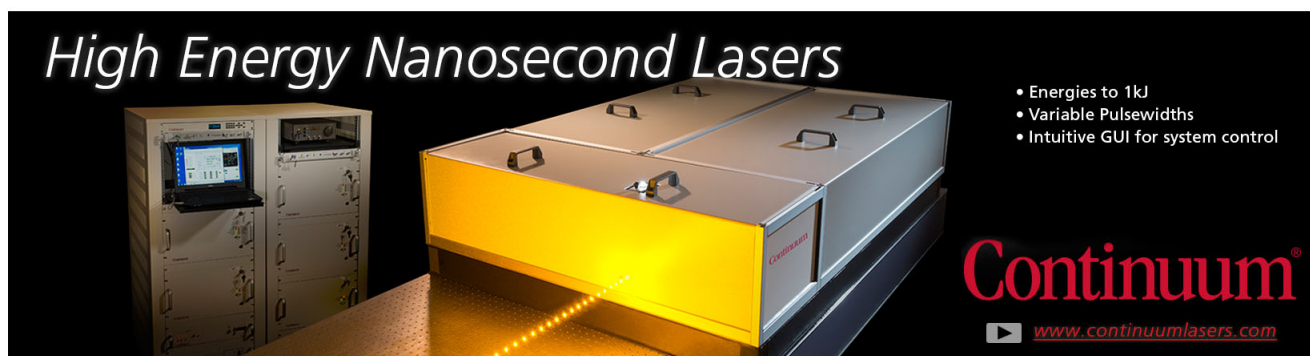
AIP Conf. Proc. **641**, 469 (2002); 10.1063/1.1521062

[Total-reflection x-ray microscopy](#)

Rev. Sci. Instrum. **72**, 2966 (2001); 10.1063/1.1374596

[Extending the methodology of X-ray crystallography to allow X-ray microscopy without X-ray optics](#)

AIP Conf. Proc. **507**, 581 (2000); 10.1063/1.1291215

The advertisement features a dark background with a photograph of a laser system. On the left is a control rack with a monitor. In the center is a large, rectangular laser unit with a glowing yellow front panel. A red laser beam is shown emanating from the bottom of the unit. The text 'High Energy Nanosecond Lasers' is written in a white, serif font at the top left. On the right, there is a list of features and the Continuum logo with the website address.

High Energy Nanosecond Lasers

- Energies to 1kJ
- Variable Pulsewidths
- Intuitive GUI for system control

Continuum[®]

www.continuumlasers.com

Correcting lateral chromatic aberrations in non-monochromatic X-ray microscopy

Ken Vidar Falch,¹ Carsten Detlefs,² Marco Di Michiel,² Irina Snigireva,² Anatoly Snigirev,³ and Ragnvald H. Mathiesen^{1,a)}

¹Department of Physics, Norwegian University of Science and Technology, Høgskoleringen 1, 7491 Trondheim, Norway

²European Synchrotron Radiation Facility, 71 Avenue des Martyrs, 38000 Grenoble, France

³Immanuel Kant Baltic Federal University, 238300 Kaliningrad, Russia

(Received 17 March 2016; accepted 21 July 2016; published online 4 August 2016)

Lateral chromatic aberration in microscopy based on refractive optics may be reduced significantly by adjustments to the illumination scheme. By taking advantage of a broadened bandwidth illumination, the proposed scheme could open for x-ray microscopy with spatial resolution in the range 150–200 nm at millisecond frame rates. The scheme is readily implemented and is achievable using only standard refractive x-ray lenses, which has the advantage of high efficiency. It also maximizes the transmission and removes the spatial filtering effects associated with absorption in x-ray lenses. *Published by AIP Publishing.* [<http://dx.doi.org/10.1063/1.4960193>]

Today microscopy experiments at synchrotrons are performed more or less exclusively with monochromatic radiation, either from a bending magnet or an undulator source. Undulator sources deliver a harmonic comb spectrum, and subsequent monochromatization filters the beam to a bandwidth typically 2–3 orders of magnitude narrower than those of the harmonic undulator peaks. Accordingly, the use of non-monochromatized undulator harmonics would yield two orders of magnitude increase in flux. This could open for new application areas, e.g., for faster structure dynamics to be addressed by *in situ* X-microscopy experiments, under the provision that challenges with increased bandwidth such as chromatic aberrations can be circumvented. The possibility of using combinations of refractive and diffractive optics to construct achromats and apochromats for visible light was pointed out already 3 decades ago.¹ It was not seriously considered for x-rays until the early 2000 s,^{2,3} with applications to x-ray telescopes in mind.⁴ More recently, microscopy based on Kirkpatrick-Baez mirrors was performed, showing negligible chromatic aberration in the 8–11 keV range, making the technique suitable for spectromicroscopy.⁵ Focusing X-ray optics is commonly based either on curved crystal mirrors,^{6–8} Fresnel zone plates,⁹ or compound refractive lenses (CRLs).¹⁰ Using CRLs for microscopy has the advantage of high efficiency, and scalability to higher energy x-rays,¹¹ which is beneficial when sample transmission is a limiting factor. While combination of CRLs with diffractive optics can be arranged to correct chromatic aberration, the introduction of a diffractive element in the microscope gives rise to a considerable loss of photons. Focal spots in the 100–200 nm range have been achieved with CRLs at 8.2 keV with a ~2% bandwidth,¹² which suggests that microscopy with similar resolution is achievable. However, when it comes to focusing, only longitudinal chromatic aberration is important. The work presented here is an investigation into

the possibility of correcting lateral chromatic aberration in microscopy purely based on CRLs.

When using a non-monochromatic beam for microscopy, the final image can be considered to be an intensity sum of images recorded with different photon energies. It can be shown that the CRL focal length, $f \propto E^2$, where E is the photon energy.¹³ Consider E_0 as the reference energy at which the microscope is in focus. Photons with energy $E \neq E_0$ will produce defocused and scaled variants of the in-focus image. The defocusing and scaling are conventionally referred to as longitudinal and lateral chromatic aberration, respectively.

Let the ray transfer matrix for the microscopy setup depicted in Figure 1(a) be

$$M = \begin{bmatrix} \mathcal{M} & \mathcal{M}d \\ \mathcal{M}c & \mathcal{M}^{-1} + dc\mathcal{M} \end{bmatrix}. \quad (1)$$

As was shown by Nazarathy and Shamir,¹⁴ the operation of a system represented by a matrix such as M on an input field is

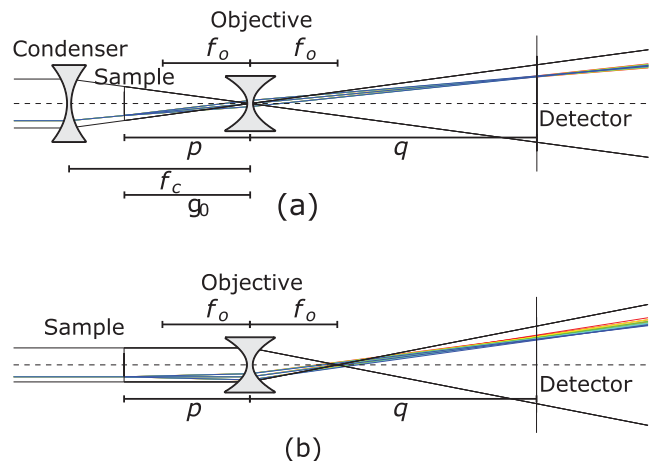


FIG. 1. (a) Microscope with beam focused into the objective lens and (b) Microscope with parallel beam illumination. Notice the distribution of the rays on the detector plane.

^{a)}Author to whom correspondence should be addressed. Electronic mail: ragnvald.mathiesen@ntnu.no

to propagate it a distance d , scaling it laterally by a factor \mathcal{M} , and applying a quadratic phase shift related to c . The latter is unimportant for imaging, provided sufficient exposure time is used. Accordingly, the energy dependence of \mathcal{M} and d is related to lateral and longitudinal chromatic aberrations, respectively. Let $\alpha = \frac{E}{E_0}$ be a measure of the deviation from the reference energy. Under the thin lens approximation

$$M = \begin{bmatrix} 1 - \frac{q}{f_0^o \alpha^2} - \frac{\left(1 - \frac{q}{f_0^o \alpha^2}\right)p + q}{f_0^c (\alpha^2 - 1) + g_0} & \left(1 - \frac{q}{f_0^o \alpha^2}\right)p + q \\ -\frac{1}{f_0^o \alpha^2} - \frac{1 - \frac{p}{f_0^o \alpha^2}}{f_0^c (\alpha^2 - 1) + g_0} & 1 - \frac{p}{f_0^o \alpha^2} \end{bmatrix}. \quad (2)$$

Here, f_0^o and f_0^c are the E_0 focal lengths of the objective and condenser lens, respectively. g_0 is the distance from the E_0 focal spot of the condenser to the sample. p and q are the distances from the objective lens to the sample and detector, respectively. Under the assumption of a narrow bandwidth, \mathcal{M} and d may be Taylor expanded about $\alpha = 1$ and $g_0 = p$ to yield

$$\mathcal{M} = \mathcal{M}_0 \left(1 - 2 \frac{\Delta g_0}{f_0^o} \Delta \alpha - 4 \frac{f_0^c}{f_0^o} \Delta \alpha^2 \right) + O(\Delta \alpha^3) + O(\Delta \alpha^2 \Delta g_0) + O(\Delta \alpha \Delta g_0^2) \quad (3)$$

and

$$\frac{d}{\alpha} = -2p \left(1 + \frac{p}{q} \right) \Delta \alpha + O(\Delta \alpha^2) + O(\Delta \alpha^2 \Delta g_0), \quad (4)$$

where $\mathcal{M}_0 = -\frac{q}{p}$, $\Delta \alpha = \alpha - 1$, and $\Delta g_0 = g_0 - p$. The motivation for expressing d/α rather than just d is to normalize the propagation distance at E to the equivalent distance at E_0 . By choosing $g_0 = p$, \mathcal{M} becomes energy independent to the first order in $\Delta \alpha$. Taylor expansion of the parallel beam case, which is obtained by letting g_0 go to infinity, results in

$$\mathcal{M} = \mathcal{M}_0 \left(1 - 2 \frac{p}{f_0^o} \Delta \alpha + 3 \frac{p}{f_0^o} \Delta \alpha^2 \right) + O(\Delta \alpha^3). \quad (5)$$

Thus, if the energy bandwidth is small, the lateral chromatic aberration can be reduced by a factor $\frac{\Delta g_0}{p}$. Eq. (4), which is also valid in the parallel beam case, shows that the longitudinal chromatic aberration at small $\Delta \alpha$ is minimized by keeping p as small as possible, and to a lesser extent by keeping $\frac{p}{q}$ as small as possible. This in turn implies that f_0^o should be relatively short. Obviously, when focal lengths become too short with respect to the length of the CRL, the thin lens approximation becomes invalid. However, the CRLs employed here are not long enough to make a significant deviation from the thin lens approximation. Therefore, a more comprehensive treatment, accounting also for lens lengths,^{13,15–18} has been omitted from Eqs. (2)–(5) but can be found as [supplementary material](#).

A test experiment has been performed at the ID06 beamline at the European Synchrotron Radiation Facility (ESRF). The output spectrum of undulator sources is dominated by a

peak at the fundamental photon energy, accompanied by odd harmonics. In the current experiment, a fundamental photon energy of 17.2 keV was used. Upstream to downstream, the setup consisted of the undulator source, a multilayer mirror, a diffuser, a condenser CRL, the sample, an objective CRL, a pair of slits, and an x-ray imaging detector. The mirror was a Ru/B₄C multilayer with a d-spacing of 5.40 nm and a bandwidth of $\frac{\Delta E}{E} = 4 \times 10^{-2}$, significantly larger than the bandwidth of the undulator peak, measured to be $\frac{\Delta E}{E} = 1.3 \times 10^{-2}$ from the power spectrum shown in Figure 2. The condenser and objective CRLs consisted of 32 and 84 double concave lenslets, respectively. Each lenslet had an apex radius of 50 μm . In the condenser, the spacing between lenslets was 2 mm, while the objective was a mix of 14×2 mm and 70×1.6 mm thick lenslets. The numerical aperture of the objective CRL was estimated to be 7.1×10^{-4} (HWHM) by a ray tracing method¹⁸ which included the physical aperture. In order to suppress speckles and smooth out features in the incident illumination, a 1.2 mm thick diffuser disc made from amorphous carbon was placed approximately 10 cm upstream of the condenser CRL. About 10 cm downstream of the objective, a pair of slits were placed. With an opening of $100 \mu\text{m} \times 100 \mu\text{m}$, the slits had no observable effect on the resolution but were useful for blocking a large portion of x-rays from the higher harmonics of the undulator. The camera was a PCO dimax CMOS, equipped with $10\times$ visible light optics and a 24.5 μm thick Eu-doped GdGa-garnet crystal scintillator. Relevant distances used were $f_0^o = 270$ mm, $q = 2600$ mm, $p = 300$ mm, and $f_0^c = 670$ mm, yielding $4f_0^c/f_0^o = 9.9$ and $d \approx 670 \text{ mm} \times \Delta \alpha$. Evaluating d at the FWHM-energies gives $d_{\text{FWHM}} = \pm 5.4$ mm. The test sample was a 4 μm thick microscopy Copper mesh with 8 μm diameter circular holes.

Figure 3 shows the experimental results with and without condenser lens. There are two main differences between the images. In the image recorded with the parallel beam (Figure 3(a)), large fringes can be seen near the edges of the holes, presumably stemming from a combination of chromatic aberration and inhomogeneous filtering in the objective lens.¹⁹ In the image recorded with the condenser (Figure 3(b)), the fringes are no longer visible. Focusing the beam into the objective lens makes the filtering homogeneous and reduces the lateral chromatic aberration. The second difference is in the radial blurring effect associated with lateral chromatic aberration. In the parallel beam case, one can see that the holes appear smeared. The smearing is almost absent

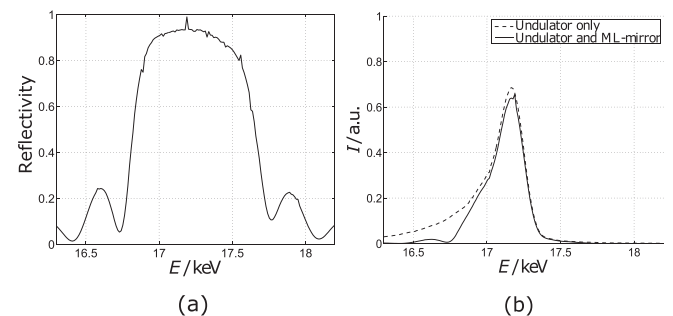


FIG. 2. (a) Measured multilayer reflectivity at the specific incident angle used in the experiment and (b) Power spectrum of the undulator and reflected spectrum.

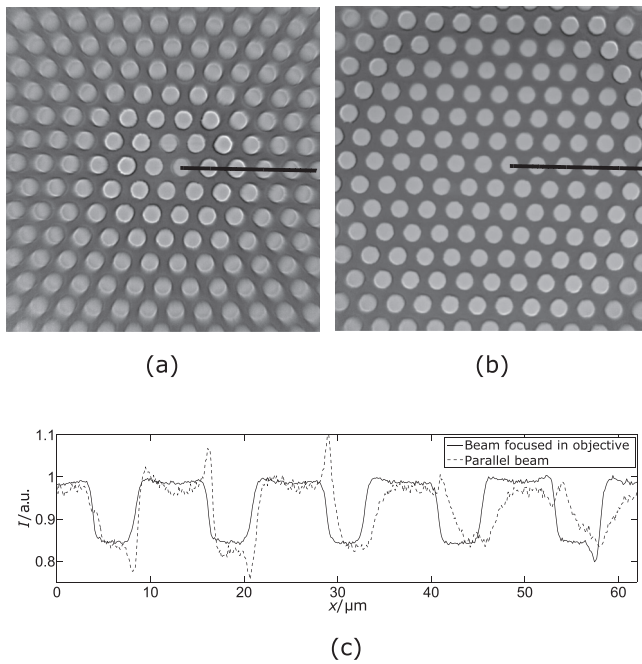


FIG. 3. (a) and (b) are images recorded with parallel illumination and with illumination focused in the objective, respectively. (c) Intensity plots sampled from the black lines in (a) and (b).

in the center of the image but becomes more and more pronounced towards the image periphery. With the beam focused in the objective, radial blurring more or less vanishes. A more intuitive physical explanation for the working principle of the suggested scheme can be found by taking into account that the angular distribution of the X-rays scattered of the sample typically is peaked in the forward direction. If the illumination is aimed at a part of the objective where it will be strongly refracted, the location of the peak in the detector plane will depend on the energy, as illustrated in Figure 1(b). By aiming the illumination at the center of the objective, as in Figure 1(a), the peaks show up in the same position in the detector for all energies. The field of view (FOV) as determined by the full width at half maximum of the illumination intensity was $113\mu\text{m}$. A drawback of the scheme is that the FOV becomes limited by the diameter of the condensed beam as opposed to the objective aperture. Larger aperture condensers are desirable for increasing the FOV.

By comparing the lines in Figure 3(c), it can be seen that there appears to be a discrepancy in the magnification of the two images. The image recorded with the parallel illumination is approximately 1.5% larger. It is not clear whether this is a real discrepancy or simply due to confusion caused by the fringes. If the microscope is perfectly focused, one would expect the magnification to be independent of the illumination. A 1.5% discrepancy would indicate that the sample was placed approximately 1.5% too far away from the objective lens, assuming that Δg is small. With $p \approx 306\text{ mm}$, this comes to 4.6 mm defocusing, which is not unreasonable considering the bandwidth. The fact that the illumination can only change the magnification if the microscope is out of focus might serve as a basis for a simple focusing algorithm. This would of course be applicable to both monochromatic and polychromatic beams.

In the corners of the image recorded with a condenser lens, one can still see that some fringes persist. This is presumably caused by illumination not focused to the correct distance, which may not be unlikely considering that the focal spot could have been slightly off. It is worth mentioning though that in the analysis presented above, no efforts have been made to account for the effects of the diffuser. It could be expected that scattering by the diffuser, in combination with a finite beam diameter, could influence the location of the effective focal spot. Further experiments would be required to determine the exact effect of the diffuser disc.

To evaluate the validity of the presented theory in practice, the microscope was replicated with a Si 111 double crystal monochromator replacing the multilayer mirror. Due to geometrical constraints, the exact distance from the sample to the detector could not be reproduced. The new distances were $p = 304\text{ mm}$ and $q = 3200\text{ mm}$, resulting in a reference magnification of $\mathcal{M}_0 = -10.4$ when the length of the objective is taken into account. Two series of images with different photon energies were recorded, one with parallel beam illumination and one with illumination focused in the objective. The results are presented in Figure 4, along with estimates based on ray transfer matrices for both thin and long lenses, following the procedure of Simons *et al.*¹⁸ The magnification of each image was estimated by measuring the distance between two features in the images. Two second order polynomials were fitted to the experimental data, and their intersection was taken as the reference length. The intersection was found at $E = 17.103\text{ keV}$. The two best focused images, judged by inspection, were found at $E = 17.10\text{ keV}$ and $E = 17.12\text{ keV}$. Note that the thin lens estimate was normalized by $\mathcal{M}_0 = -10.5$ which is slightly larger in magnitude than in the long lens case. The experimental curves fit well to the ray trace estimates. In the focused beam case, the largest discrepancies between model and polynomial fit can be attributed to Δg_0 being in the range of 30–40 mm. It is evident that long lens calculations give an improved fit for the parallel beam case. In conclusion, the principle behind the presented lateral chromatic aberration correction scheme appears to be valid.

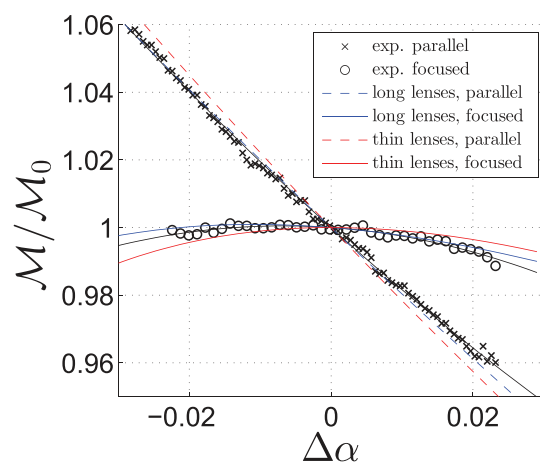


FIG. 4. Theoretical and experimentally determined magnification of images at different photon energies. The black curves are second order polynomial fits.

See [supplementary material](#) for calculation of long lens relative magnification.

The authors would like to acknowledge the Norwegian Research Council (Project Grant No. 218404/F50), the Ministry of Education and Science of the Russian Federation (Contract No. 14.Y26.31.0002) and the European Synchrotron Radiation Facility for supporting this work.

¹T. Stone and N. George, *Appl. Opt.* **27**, 2960 (1988).

²G. K. Skinner, *AIP Conf. Proc.* **587**, 855 (2001).

³G. K. Skinner, *Appl. Opt.* **43**, 4845 (2004).

⁴G. K. Skinner, Z. Arzoumanian, W. C. Cash, N. Gehrels, K. C. Gendreau, P. Gorenstein, J. F. Krizmanic, M. C. Miller, J. D. Phillips, R. D. Reasenberg, C. S. Reynolds, R. M. Sambruna, R. E. Streitmatter, and D. L. Windt, *Proc. SPIE* **7011**, 70110T (2008).

⁵S. Matsuyama, Y. Emi, H. Kino, Y. Kohmura, M. Yabashi, T. Ishikawa, and K. Yamauchi, *Opt. Express* **23**, 9746 (2015).

⁶O. Hignette, P. Cloetens, G. Rostaing, P. Bernard, and C. Morawe, *Rev. Sci. Instrum.* **76**, 063709 (2005).

⁷W. J. Liu, G. E. Ice, J. Z. Tischler, A. Khounsary, C. Liu, L. Assoufid, and A. T. Macrander, *Rev. Sci. Instrum.* **76**, 113701 (2005).

⁸H. Mimura, S. Handa, T. Kimura, H. Yumoto, D. Yamakawa, H. Yokoyama, S. Matsuyama, K. Inagaki, K. Yamamura, Y. Sano, K.

Tamasaku, Y. Nishino, M. Yabashi, T. Ishikawa, and K. Yamauchi, *Nat. Phys.* **6**, 122 (2010).

⁹W. L. Chao, B. D. Harteneck, J. A. Liddle, E. H. Anderson, and D. T. Attwood, *Nature* **435**, 1210 (2005).

¹⁰C. G. Schroer, F. E. Brack, R. Brendler, S. Honig, R. Hoppe, J. Patommel, S. Ritter, M. Scholz, A. Schropp, F. Seiboth, D. Nilsson, J. Rahomaki, F. Uhlen, U. Vogt, J. Reinhardt, and G. Falkenberg, *Proc. SPIE* **8848**, 884807 (2013).

¹¹S. D. Shastri, P. Kenesei, and R. M. Suter, *Proc. SPIE* **9592**, 95920X (2015).

¹²F. Seiboth, A. Schropp, R. Hoppe, V. Meier, J. Patommel, H. J. Lee, B. Nagler, E. C. Galtier, B. Arnold, U. Zastra, J. B. Hastings, D. Nilsson, F. Uhlen, U. Vogt, H. M. Hertz, and C. G. Schroer, in Proceedings of the 22nd International Congress on X-Ray Optics and Microanalysis (2014), Vol. 499, p. 012004.

¹³B. Lengeler, C. Schroer, J. Tummler, B. Benner, M. Richwin, A. Snigirev, I. Snigireva, and M. Drakopoulos, *J. Synchrotron Radiat.* **6**, 1153 (1999).

¹⁴M. Nazarathy and J. Shamir, *J. Opt. Soc. Am.* **72**, 356 (1982).

¹⁵V. G. Kohn, *JETP Lett.* **76**, 600 (2002).

¹⁶V. G. Kohn, *J. Exp. Theor. Phys.* **97**, 204 (2003).

¹⁷I. I. Snigireva, V. G. Kohn, and A. A. Snigirev, *Proc. SPIE* **5539**, 218 (2004).

¹⁸H. Simons, F. Stohr, J. Michael-Lindhard, F. Jensen, O. Hansen, C. Detlefs, and H. F. Poulsen, *Opt. Commun.* **359**, 460 (2016).

¹⁹C. G. Schroer, B. Benner, T. F. Gunzler, M. Kuhlmann, B. Lengeler, C. Rau, T. Weitkamp, A. Snigirev, and I. Snigireva, *Proc. SPIE* **4503**, 23 (2002).